

Fermi Surface of the 2D Hubbard Model at Weak Coupling

Christoph J. Halboth and Walter Metzner

Sektion Physik, Universität München

Theresienstraße 37, D-80333 München, Germany

October 30, 1996

Abstract

We calculate the interaction-induced deformation of the Fermi surface in the two-dimensional Hubbard model within second order perturbation theory. Close to half-filling, interactions enhance anisotropies of the Fermi surface, but they never modify the topology of the Fermi surface in the weak coupling regime.

PACS: 05.30.Fk, 71.10.Fd, 71.18.+y

1 Introduction

Since the discovery of high-temperature superconductivity, the structure of low-lying single-particle excitations in two-dimensional interacting Fermi systems has attracted much interest [1, 2]. A key role is thereby played by the shape of the Fermi surface which determines the phase space for residual scattering processes and thus decay rates and Fermi liquid instabilities [3]. In a recent Monte Carlo simulation of the two-dimensional Hubbard model Bulut, Scalapino and White [4] have found that strong interactions may not only deform the Fermi surface of the non-interacting reference system, but may even lead to a different topology. While the Fermi surface of the non-interacting Hubbard model (with next-neighbor hopping) is always closed around the origin in \mathbf{k} -space for densities $n < 1$, the strongly interacting system exhibited a Fermi surface closed around (π, π) for densities close to but below half-filling. This result raises the interesting question whether such a behavior occurs only in a strong coupling regime. Zlatić, Schotte and Schliecker [5] have recently argued that the Fermi surface topology can be changed by arbitrarily weak interactions in the limit $n \rightarrow 1$, since in that limit arbitrarily small deformations could lead to a topologically different shape.

In the following we will analyze the interaction-induced deformation of the Fermi surface in the two-dimensional Hubbard model within second order perturbation theory. We show that interactions enhance the anisotropy of the Fermi surface for densities close to half-filling, but they do not change the topology by deforming a $(0, 0)$ -centered surface into a (π, π) -centered one in the weak coupling regime.

2 Fermi Surface and Perturbation Expansion

The Hubbard model Hamiltonian is given by

$$H = -t \sum_{\sigma} \sum_{\langle j, j' \rangle} c_{j'\sigma}^\dagger c_{j\sigma} + U \sum_j n_{j\uparrow} n_{j\downarrow} \quad (1)$$

where t is the next-neighbor hopping amplitude and U the on-site Coulomb repulsion. The operators $c_{j\sigma}^\dagger$ ($c_{j\sigma}$) create (annihilate) fermions with spin projection σ on lattice site j and $n_{j\sigma} = c_{j\sigma}^\dagger c_{j\sigma}$.

The non-interacting band-structure for next-neighbor hopping on a square lattice is

$$\epsilon_{\mathbf{k}}^0 = -2t(\cos k_x + \cos k_y) \quad (2)$$

This leads to a strictly convex Fermi surface centered around $\mathbf{k} = (0, 0)$ for densities $n < 1$, to a diamond shaped surface at half-filling ($n=1$), and a (π, π) -centered Fermi surface for densities $n > 1$ (see Fig. 1).

The Fermi surface of the interacting system can be obtained from the one-particle Green function

$$G(\mathbf{k}, \omega) = \frac{1}{\omega - (\epsilon_{\mathbf{k}}^0 - \mu) - \Sigma(\mathbf{k}, \omega)} \quad (3)$$

where $\Sigma(\mathbf{k}, \omega)$ is the self-energy. The chemical potential μ controls the average particle density n . The equation

$$\text{Re } G^{-1}(\mathbf{k}, \omega) = \xi_{\mathbf{k}} - (\epsilon_{\mathbf{k}}^0 - \mu) - \text{Re } \Sigma(\mathbf{k}, \xi_{\mathbf{k}}) = 0 \quad (4)$$

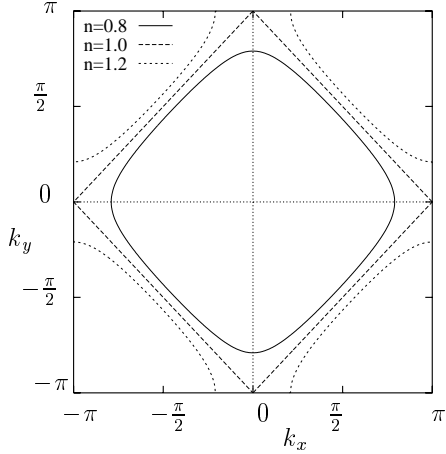


Figure 1: The Fermi surface of the non-interacting system ($U = 0$) for various densities n .

determines the energy $\xi_{\mathbf{k}} \equiv \epsilon_{\mathbf{k}} - \mu$ of coherent single-particle excitations (quasi-particles) in the interacting system [6]. The Fermi surface is the set of those points in \mathbf{k} -space where the excitation energy vanishes, i.e. $\xi_{\mathbf{k}_F} = 0$, and thus determined by

$$\epsilon_{\mathbf{k}_F}^0 - \mu + \text{Re } \Sigma(\mathbf{k}_F, 0) = 0 \quad (5)$$

According to the Luttinger theorem [7], the volume enclosed by the Fermi surface is related to the particle density by

$$n = 2 \int \frac{d^2 k}{(2\pi)^d} \Theta(\mu - \epsilon_{\mathbf{k}}) \quad (6)$$

We now calculate the interaction induced deformation of the Fermi surface to second order in the coupling strength U . The particle density is kept fixed by a suitable choice of an interaction-dependent chemical potential $\mu = \mu(n, U) = \mu_0 + \delta\mu$, where $\mu_0 = \mu_0(n)$ is the chemical potential corresponding to density n at $U = 0$. We denote the Fermi wave vectors of the non-interacting system by \mathbf{k}_{F0} and the deformation vectors by $\delta\mathbf{k}_F = \mathbf{k}_F - \mathbf{k}_{F0}$.

To first order in U , the self-energy is a real constant: $\Sigma_1(\mathbf{k}, \omega) = Un/2$. To keep the density fixed, the chemical potential has to be shifted accordingly by $\delta\mu_1 = Un/2$, which cancels Σ_1 completely in G .

To second order in U , two Feynman diagrams contribute to the self-energy of the Hubbard model (see Fig. 2). The second one is a real constant which is completely cancelled by a corresponding shift of the chemical potential.¹ The first diagram, however, leads to a \mathbf{k} -dependent

¹We note that this diagram is "anomalous" in the sense of Kohn and Luttinger [8], i.e. it vanishes if the thermodynamic limit is taken strictly at $T = 0$, while it yields a finite contribution if the zero temperature limit is taken after the thermodynamic limit.

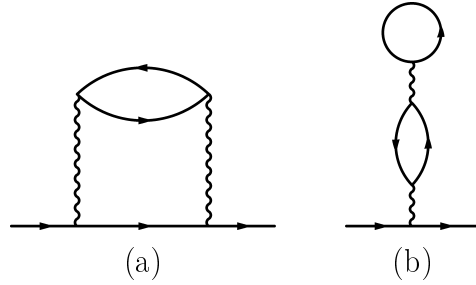


Figure 2: Feynman diagrams contributing to the second order self-energy.

contribution and generates a Fermi surface deformation. Expanding Eqs. (5) and (6) with $\mathbf{k}_F = \mathbf{k}_{F0} + \delta\mathbf{k}_F$ and $\mu = \mu_0 + \delta\mu$ in powers of U and comparing the second order terms, one obtains the relation

$$\nabla \epsilon_{\mathbf{k}_{F0}}^0 \cdot \delta\mathbf{k}_{F2} = \delta\mu_2 - \Sigma_2(\mathbf{k}_{F0}, 0) \quad (7)$$

for the deformation of the Fermi surface to second order in U , where the chemical potential shift is given by the Fermi surface average

$$\delta\mu_2 = \frac{\int d^2 k \delta(\epsilon_{\mathbf{k}}^0 - \mu) \Sigma_2(\mathbf{k}, 0)}{\int d^2 k \delta(\epsilon_{\mathbf{k}}^0 - \mu)} \quad (8)$$

Note that Σ_2 is real at zero frequency. Of course there are many ways to define a map $\mathbf{k}_{F0} \mapsto \mathbf{k}_F$ between non-interacting and interacting Fermi surfaces. A natural choice is $\delta\mathbf{k}_F = \delta k_F \mathbf{n}_{\mathbf{k}_{F0}}$, where $\mathbf{n}_{\mathbf{k}_{F0}}$ is a unit vector normal to the non-interacting Fermi surface in \mathbf{k}_{F0} . Eq. (7) then determines the modulus of the shift as

$$\delta k_{F2} = \delta k_{F2}(\mathbf{k}_{F0}) = \frac{\delta\mu_2 - \Sigma_2(\mathbf{k}_{F0}, 0)}{v_{\mathbf{k}_{F0}}^0} \quad (9)$$

where $v_{\mathbf{k}_{F0}}^0 = |\nabla \epsilon_{\mathbf{k}_{F0}}^0|$ is the Fermi velocity of the non-interacting system.

The second order self-energy has not yet been evaluated by purely analytical means. Using the spectral representation of the non-interacting propagator G_0 , one can write the imaginary part of the self-energy contribution associated with the first Feynman diagram in Fig. 2 as

$$\begin{aligned} \text{Im} \Sigma_{2a}(\mathbf{k}, \omega) &= -\frac{\text{sgn}(\omega)}{\pi} U^2 \int \frac{d^2 q}{(2\pi)^2} \int_0^\omega d\nu \\ &\quad \text{Im} \Pi_0(\mathbf{q}, \nu) \text{Im} G_0(\mathbf{k} - \mathbf{q}, \omega - \nu) \end{aligned} \quad (10)$$

where the imaginary part of the non-interacting polarisation bubble is given by

$$\begin{aligned} \text{Im} \Pi_0(\mathbf{q}, \nu) &= \frac{\text{sgn}(\nu)}{\pi} \int \frac{d^2 p}{(2\pi)^2} \int_{-\nu}^0 d\omega' \\ &\quad \text{Im} G_0(\mathbf{p}, \omega') \text{Im} G_0(\mathbf{p} + \mathbf{q}, \omega' + \nu) \end{aligned} \quad (11)$$

and $\text{Im}G_0(\mathbf{k}, \omega) = -\pi \text{sgn}(\omega) \delta[\omega - (\epsilon_{\mathbf{k}}^0 - \mu_0)]$. Performing the integrals over ω' , p_x and q_x in (10) and (11) analytically (eliminating thus three δ -functions), one obtains the expression

$$\begin{aligned} \text{Im}\Sigma_{2a}(\mathbf{k}, \omega) &= -\text{sgn}(\omega) \frac{U^2}{64\pi^3 t^2} \int dq_y \int dp_y \int_0^\omega d\nu \\ &\quad \sum_{q_x^0, p_x^0} \left[\frac{\Theta(\mu_0 - \epsilon_{\mathbf{p}}^0) - \Theta(\mu_0 - \epsilon_{\mathbf{p}+\mathbf{p}}^0)}{\sqrt{(1-f^2)(4\sin^2(q_x/2) - g^2)}} \right] \quad (12) \end{aligned}$$

with the functions

$$\begin{aligned} f &= (\nu - \omega - \mu_0)/2t - \cos(k_y - q_y) \\ g &= \nu/2t + \cos(p_y + q_y) - \cos(p_y) \end{aligned} \quad (13)$$

The summation variables q_x^0 and p_x^0 in (12) are the roots of the set of equations

$$\begin{aligned} \cos(k_x - q_x) &= f \\ 2 \sin(p_x + q_x/2) \sin(q_x/2) &= g \end{aligned} \quad (14)$$

The remaining three-fold integral is easily computed numerically (e.g. via a standard Monte-Carlo routine on a work-station). Note that the representation in (12) is particularly suitable for a high resolution of the low-energy limit $\omega \rightarrow 0$, since the integration region shrinks with ω . The full self-energy function can be reconstructed from its imaginary part $\text{Im}\Sigma_{2a}$ by a simple Hilbert transform

$$\Sigma_{2a}(\mathbf{k}, \omega) = -\pi^{-1} \int_{-\infty}^{\infty} d\omega' \frac{|\text{Im}\Sigma_{2a}(\mathbf{k}, \omega')|}{\omega - \omega' + i0^+ \text{sgn}(\omega)} \quad (15)$$

The constant contribution Σ_{2b} from the second diagram in Fig. 2 need not be calculated since it is completely cancelled by a corresponding shift $\delta\mu_{2b}$ of the chemical potential. Our numerical results for the second order self-energy agree with those published recently by Zlatić et al. [5], who computed Σ_{2a} via a sequence of fast Fourier transforms. They also agree with earlier results by Schweitzer and Czycholl [9] and by Ossadnik [10].

3 Results for the Fermi Surface Deformation

To discuss explicit results for the Fermi surface deformation we introduce polar coordinates in \mathbf{k} -space. Points on the Fermi surface of the non-interacting system are thus specified by an angle ϕ . Due to the discrete symmetries of the square lattice it is sufficient to consider angles between 0 and 45 degrees. In Fig. 3 we show results for $\delta k_{F2}/U^2$ as a function of ϕ for various densities n . Here and in the following we set the hopping amplitude $t = 1$. At low densities $n < 0.6$ weak interactions

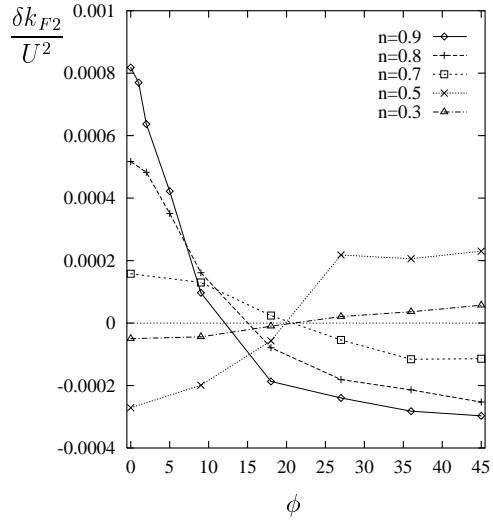


Figure 3: Shifts of the Fermi surface $\delta k_{F2}/U^2$ as a function of the angle ϕ for various densities n .

tend to compensate anisotropies of the non-interacting Fermi surface while at densities $0.7 < n < 1$ anisotropies are further enhanced by interactions, as observed already earlier in unpublished work by Ossadnik [10]. The diamond shaped Fermi surface at half-filling is of course not affected at all by interactions, as a consequence of the particle-hole symmetry of the Hubbard model (1). More generally, particle-hole symmetry maps the Fermi surface at density n onto the surface for density $2 - n$ by a simple (π, π) -shift in \mathbf{k} -space (the diamond at half-filling is thereby mapped onto itself).

Let us now clarify whether weak interactions can modify the Fermi surface topology at densities close to half-filling. The first Fermi point that may reach the Brillouin zone boundary (and thus introduce a different topology) upon increasing U is obviously the one at $\phi = 0$, since it is closer to the zone boundary than any other Fermi point already in the non-interacting system and in addition $\delta k_F(\phi)$ is maximal for $\phi = 0$ (if $n > 0.7$). Quantitative information on the Fermi surface deformation in the "critical" regime $n \rightarrow 1$ and $\phi \rightarrow 0$ is provided in Fig. 4, where we have plotted $\delta k_{F2}/U^2$ as a function of density for various small angles ϕ . Within numerical accuracy, $\delta k_{F2}(\phi)$ tends to 0 for $n \rightarrow 1$ for all ϕ , as expected from particle-hole symmetry and continuity. Finally, in Fig. 5 we show the critical coupling strength $U_c(n)$ that is required to make $\mathbf{k}_F = \mathbf{k}_{F0} + \delta\mathbf{k}_{F2}$ reach the Brillouin zone boundary (at the point $(\pi, 0)$). Close to half-filling, $U_c(n)$ behaves linearly as a function of density and extrapolates to a rather big *finite* value in the limit $n \rightarrow 1$. Hence,

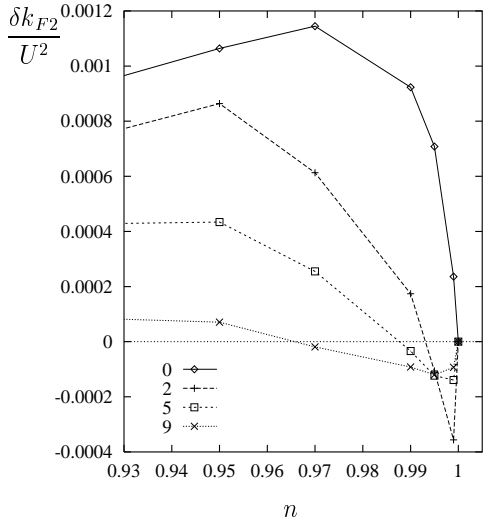


Figure 4: $\delta k_{F2}/U^2$ as a function of n (close to half-filling) for various small angles ϕ .

interactions do not modify the Fermi surface topology of the two-dimensional Hubbard model within the perturbatively controlled weak coupling regime at any density.

Zlatić et al. have calculated the critical coupling strength from second order perturbation theory for $n = 0.97$ (only), where they obtained a smaller U_c (by a factor of about 2) than we did, although our results for the self-energy agree. The discrepancy arises because these authors have determined the new Fermi surface by directly solving Eq. (5) with the second order self-energy, while we have expanded δk_F to second order in U , which is the order we really control. In the small U limit both procedures yield the same shift to order U^2 , but quantitative differences arise for finite U . The qualitative result that $U_c(n)$ remains finite in the limit $n \rightarrow 1$ is thereby not affected.

In summary, we have calculated the interaction-induced deformation of the Fermi surface in the two-dimensional Hubbard model within second order perturbation theory. Close to half-filling, interactions enhance anisotropies of the Fermi surface, but they never modify the topology of the Fermi surface in the weak coupling regime.

Acknowledgement We are very grateful to Dieter Vollhardt for numerous valuable discussions.

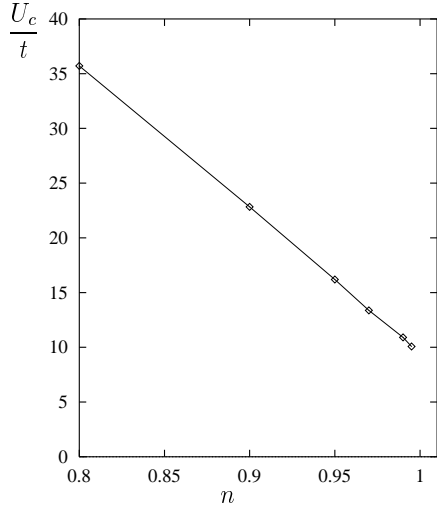


Figure 5: Critical coupling $U_c(n)$ required to change the topology of the Fermi surface.

References

- [1] See, for example, Proceedings of the International Conference on *Materials and Mechanisms of Superconductivity: High Temperature Superconductors IV*, ed. P. Wyder (North Holland 1994).
- [2] For a review of numerical results, see E. Dagotto, Rev. Mod. Phys. **66**, 763 (1994).
- [3] For a review on the Fermi surface structure and other properties of high- T_c superconductors, see W.E. Pickett, H. Krakauer, R.E. Cohen and D.J. Singh, Science **255**, 46 (1992).
- [4] N. Bulut, D.J. Scalapino and S.R. White, Phys. Rev. B **50**, 7215 (1994).
- [5] V. Zlatić, K.D. Schotte and G. Schliecker, Phys. Rev. B **52**, 3639 (1995).
- [6] A.A. Abrikosov, L.P. Gorkov, and I.E. Dzyaloshinskii, *Methods of Quantum Field Theory in Statistical Physics* (Dover, New York 1975).
- [7] J.M. Luttinger, Phys. Rev. **119**, 1153 (1960).
- [8] W. Kohn and J.M. Luttinger, Phys. Rev. **118**, 41 (1960).
- [9] H. Schweitzer and G. Czycholl, Z. Phys. B **83**, 93 (1991).
- [10] P. Ossadnik, Diploma Thesis (Universität Köln 1990).